Tribological Evaluation of Ferritic-Austenitic Stainless Steel Coatings with Different Percentages of Silver

Claudia Liliana España Peña[a,b], Jhon Jairo Olaya Flórez[a]* , Abel André Cândido Recco[c]

[a]Universidad Nacional de Colombia, Departamento de Ingeniería Mecánica Y Mecatrónica, 111321, Bogotá, Colombia.
[b]Corporación Universitaria Comfacauca (Unicomfacauca), Faculdade de Engenharia, Popayán, Colombia.
[c]Universidade do Estado de Santa Catarina (UDESC), Departamento de Física, 89219-710, Joinville, Brasil.

Stainless steels have been evaluated in the form of coatings or thin films deposited using magnetron sputtering in various investigations. In most of these investigations, mainly the microstructural evaluation of this type of coating has been reported, while the evaluation of wear resistance has not been widely studied. In the present investigation, **ferritic-austenitic** stainless steel coatings with different percentages of silver were deposited by means of unbalanced DC magnetron sputtering. A stainless steel target doped with different numbers of silver inserts (0, 1, 2, 3, and 4 inserts) was used, obtaining coatings with silver percentages of up to 7.7 at. %, in order to evaluate their tribological properties. During the synthesis, the first layer of the bilayer was deposited with argon and the other in an atmosphere of argon and nitrogen. The structure of the coatings was evaluated by use of X-ray diffraction (XRD), and the morphology and the chemical composition were studied by means of scanning electron microscopy (SEM) and energy-dispersive X-ray spectroscopy (EDS), respectively. The hardness was tested through nanoindentation, and the wear test was carried out using the pin-on-disc technique. The wear tracks were evaluated via profilometry, SEM, and EDS. In general, the deposited films exhibited BCC and FCC phases and a compact morphology, as well as good adherence to the substrate. The results of the evaluation of the mechanical properties revealed an increase in the hardness of the coatings when the silver content was augmented, obtaining values of 9.8 GPa and 12.1 GPa for coatings with 0 and 4 silver inserts, respectively. Likewise, it was found that the wear resistance of coatings was higher, up to two orders of magnitude compared to the 316L stainless steel substrate. Finally, the wear rate of the multilayers decreased slightly with an increase in the percentage of silver in the films produced, up to an order of magnitude for the coating with 4 silver inserts relative to the coating with 0 silver inserts.

Keywords: *Multilayer, stainless Steel, wear, sputtering.*

1. Introduction

Physical vapor deposition (PVD) techniques are widely used to obtain coatings with properties superior to conventional materials. Among the coatings that can be obtained by PVD are multilayer coatings, which are characterized by moderate residual stresses, good adhesion to metal substrates, adequate hardness and toughness, and low coefficients of friction. This type of multilayer structure can be obtained with a great variety of materials and any number of layers, according to the requirements of the application. On the other hand, austenitic stainless steels are materials that are widely used in various applications, due to their properties such as resistance to corrosion and good formability. Their use in applications such as biomaterials is one of the most common ones, due to having a good combination of biological and anticorrosive properties that make them suitable for use in orthopedics[1].

The one most widely employed is 316L stainless steel, which is characterized by exhibiting a face-centered cubic crystalline structure (FCC)[2] in addition to exhibiting a thin oxide film on the surface, making it suitable for applications where high resistance to corrosion is required[3,4] . However, it has been found that 316L steel presents difficulties in some of its biomedical applications, due to the fact that the mechanical properties are often insufficient, as well as its low resistance to wear, the latter being an essential property in biomedical applications (prostheses, kneecaps, etc.) for which an improvement in this property is necessary[5].

The investigations that have been carried out have evaluated the synthesis of stainless steel coatings by means of sputtering techniques finding that this type of coating exhibits compositions similar to those of the target, with a variation in the crystalline structure obtained, from an FCC structure in the target to a body-centered cubic (BCC) one for coatings obtained in inert atmospheres composed of argon.

As an alternative, the production of stainless steel coatings in reactive atmospheres with the presence of nitrogen has been investigated[6-9]. It has been found that nitrogen stabilizes the FCC structure, depending on the concentration of gas used, as well as the temperature of the substrate. In this way, it is possible to obtain coatings with higher hardness values and better resistance to corrosion in comparison with conventional bulk stainless steels[10-12]. On the other hand, silver (Ag) is a metallic material that has been highly investigated and used in recent decades in biomedical applications, due to its antibacterial properties, providing anti-infectious characteristics to biomedical devices[13-14]. Coatings doped with silver are characterized by having good tribological and antibacterial properties and are of interest where high resistance to wear and low coefficient of friction are required, as well as protection against microbial agents[15]. Such is the case of silver-doped titanium carbonitride (TiCN) coatings, which have exhibited better wear behavior and decreased wear rate and friction coefficient when silver percentages up to 6 at. % are used. Likewise, TiSiN coatings showed good wear behavior with up to 8.7 at. % Ag. The wear resistance of coatings containing silver is attributed to the possible performance of silver as a solid lubricant on the surface where these coatings are used, leading to an increase in their wear resistance[16-18]. Similarly, other researchers have evaluated the wear resistance of stainless steel coatings, showing a decrease in the wear rate values compared to the uncoated substrate[9,19-21]. However, we were not able to find a paper related to the wear resistance of ferritic-austenitic stainless steel coatings to be used in biomedical applications within the scientific literature. For that reason, this article is focused on the study of the tribological evaluation of silver-doped stainless steel coatings produced by sputtering, in which the first bilayer was deposited with argon and the other in an atmosphere of argon-nitrogen. In this case, nitrogen was used in order to obtain coatings with FCC or BCC crystalline structures.

2. Experimental Details

Stainless steel multilayer coatings were deposited using the unbalanced DC magnetron sputtering technique from a 4-inch diameter 316L stainless steel target. The equipment used consisted of a cylindrical stainless steel chamber with a removable cover for the entry of the substrates to be coated on which both the magnetron and the target to be used were located (see diagram in Figure 1). In order to achieve the vacuum inside the chamber, two pumps were used, one mechanical and one turbomolecular. The sputtering equipment used a direct current source and also had a cooling system (with water) in order to protect the magnetron from possible overheating. The heating of the substrates was carried out using a set of halogen lamps with a power of 250W each. To control the temperature, a microcontroller connected to a type K thermocouple was used.

The coatings were deposited on polished silicon (100) and 316L stainless steel substrates, which were subsequently cleaned with acetone and ethanol using an ultrasound machine for 10 minutes. 4x4 mm square pieces of high-purity silver (Ag) were used, which were in the zone of greatest erosion of the stainless steel target, as shown in Figure 2. In order to vary the silver content in the coatings, different numbers of pieces (0, 1, 2, 3, and 4 pieces) were used.

The working pressure was approximately 0.2 Pa, the substrate temperature was 300 °C, and a power density of 7 W/cm^2 was used. The multilayers were grown for the same period of time in an inert atmosphere and in a reactive atmosphere. The first layer was deposited in an inert argon atmosphere, followed by a layer deposited in an argon and nitrogen atmosphere, to produce coatings with a total of 8 bilayers, as shown in the diagram of Figure 3. During the discharge, the power density remained constant, while the voltage and current remained between the values of 570 V and 580 V and 0.95 A and 1.05 A, respectively. The argon flow was 2.0×10^{-8} cubic meter per second (m^3/s) and that of the N_2 was 1.3×10^{-8} cubic meter per second (m^3/s). The deposition time of the coatings was calculated to obtain thicknesses of approximately 4 micrometers, which were determined by means of a Bruker DektakXT profilometer (Billerica, MA, USA). For this purpose, a smaller segment of this same material was placed on a silicon substrate in order to generate a step, which was later measured in order to obtain the thickness of the coating. The coatings were
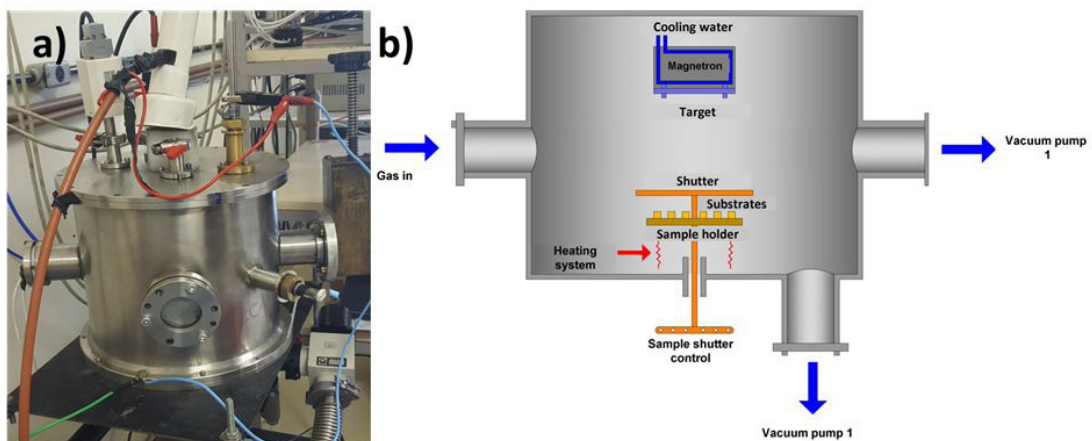
Figure 1. (a) Photography and (b) scheme of the sputtering equipment used for film deposition.

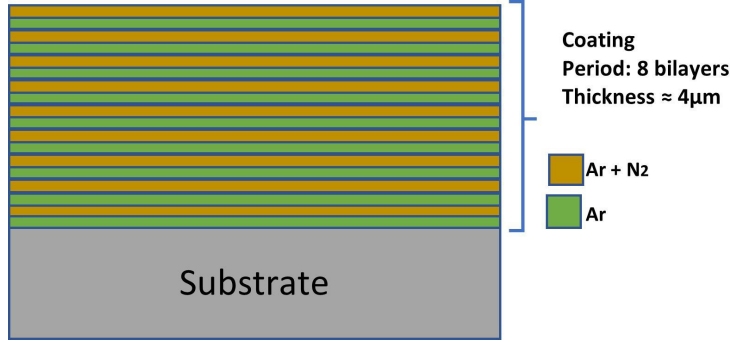**Figure 2.** 316L stainless steel (SS316L) target doped with inserts of Ag (0, 1, 2, 3, and 4 inserts).

Figure 3. Diagram of the proposed bilayers that made up the deposited coatings.

Table 1. Parameters obtained by means of XRD for coating deposited. D is grain size, ε is deformation percentage, and a is lattice parameter.

Multilayer	Phase	Reflection (h k l)	D (nm)	ε	a (nm)
M0	α-Fe	110	12.31	0.13	0.288
	γ-Fe	200	10.12	0.19	0.363
M1	α-Fe	110	11.41	0.14	0.288
	γ-Fe	200	8.99	0.22	0.363
M2	α-Fe	110	5.46	0.29	0.285
	γ-Fe	200	8.50	0.21	0.362

designated, as shown in Table 1, as M0, M1, M2, M3, and M4, according to the number of Ag pieces used: 0, 1, 2, 3, or 4.

The morphology of the coatings was evaluated by means of scanning electron microscopy using a JEOL JSM model 7600F microscope, and the chemical composition was determined via energy-dispersive X-ray spectroscopy using Shimadzu EDX-720 equipment, which allows detecting elements from Na (Z = 11) to U (Z = 90). The structural analysis of the coatings was carried out by means of X-ray diffraction using an X'pert PRO PANalytical diffractometer, working in the grazing beam mode, with monochromatic radiation Kα of copper λ = 1.542 Å, with a current intensity of 40 mA, and a 45 KV potential difference. The sweep range was 35° to 85° in 2Θ mode, with a step size of 0.02° in continuous mode. The crystallite size was determined by the Scherrer formula, as shown in Equation 1[22] , where λ is the X-ray wavelength used in the experiment, B is the peak broadening at half maximum intensity in radians (taking into account the subtraction of the experimental error of the measuring equipment, Bexp), θ is the Bragg angle, and k is a constant related to the shape factor (0.94).

$$Grain\,size = \frac{k\lambda}{Bcos\theta} \qquad (1)$$

The hardness and the elastic modulus of the multilayers were determined by means of nanoindentation measurements, using CTER Nano-Micro nanoindenter equipment, which employs a Berkovich-type tip, applying a maximum load of 10 μN, and the maximum penetration depth of the tip did not exceed 10% of the coatings' thickness, in order to eliminate the contribution of the substrate to the measurements. The adhesion of the coatings to the substrate was evaluated by means of the scratch test technique, using a CSM Instruments model Revetest Xpress. A progressive load from 1 to 60N was applied. The scratch track was analyzed by means of optical microscopy.

The tribological properties of the produced coatings were determined using a CETR-UMC-2-110 tribometer through pin-on-disk tests, at room temperature, and with a relative humidity of 60%. A 6mm diameter alumina ball was used, with a load of 1N and a speed of 10 mm/s for 10 minutes. The wear volume (Wv) of the films was calculated according to ASTM G99-17[23]. The wear track cross profile was measured at at least four points of the wear track with a Dektak 150 profilometer (Bruker, Billerica, MA, USA) in order to obtain an average of the wear track width. After the test, the wear tracks were examined using a Bruker contour GT optical profilometer. The wear products were chemically analyzed using energy-

dispersive X-ray spectroscopy (EDS). The wear rate (Ws) was calculated according to Archard's equation, Equation 2[24], where F is the normal load (N) and L is the sliding length (mm). The wear rate is reported in mm³/Nm.

$$W_s = \frac{W_v}{F \cdot L} \qquad (2)$$

3. Results and Discussion

The X-ray diffraction patterns of the stainless steel coatings with different silver contents are shown in Figure 4. The coatings M0 and M1 exhibited the same diffraction peaks, where the signal (100) is associated with the ferritic phase (α-Fe) and peak (200) is related to the austenitic phase (γ-Fe) of stainless steel[25-28]. In investigations on the deposition of stainless steel coatings deposited in an inert atmosphere composed solely of argon, it has been found that the structure obtained is BCC (ferritic phase) while the FCC structure (austenitic phase) is obtained by depositing this type of coating in reactive atmospheres in the presence of nitrogen (Ar + N$_2$), because the nitrogen tends to stabilize the FCC structure by broadening the gamma loop in the iron-carbon equilibrium diagram, which has been reported by other researchers[10-12]. Nevertheless, the increase in the silver content in the films (samples M2, M3, and M4) results in a decrease in the intensity of peak (200)
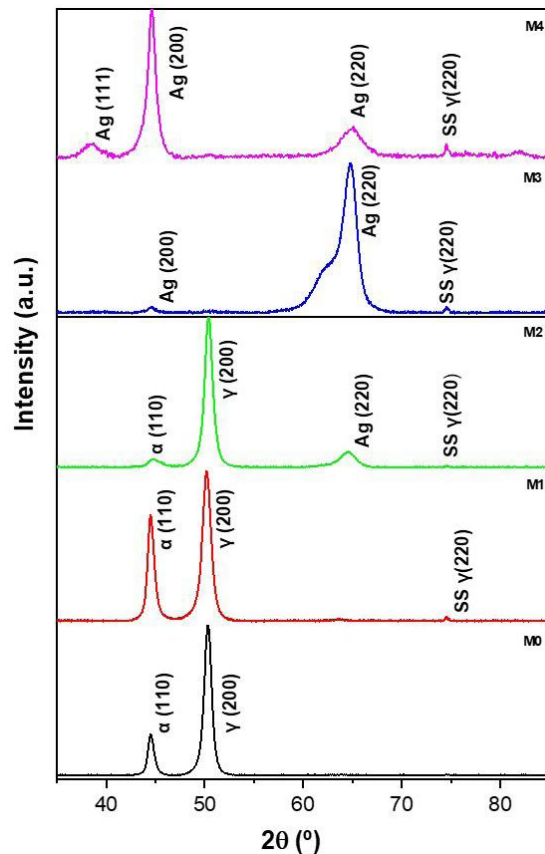
associated with the austenitic phase (FCC structure) of the stainless steel coating, which may be related to a possible to a amorphization effect due to to the inhibition of grain growth[16]. On the other hand, peaks (111) and (220) can be seen in the coatings with the highest percentage of Ag (M4), which is associated with the FCC structure of silver[18,29,30]. Regarding sample M3, it is possible to identify an atypical behavior compared to the other coatings, where there is a phenomenon of preferential orientation change, possibly due to a change in the surface energy and formation of the monolayers that make up the coatings' behavior , which will be evaluated through subsequent complementary studies. Besides, the silver incorporated in the coatings could be in the form of nanoparticles or embedded in the steel-film crystal boundary, according to the characteristics of the peaks identified in the diffractograms of the coatings obtained. However, additional studies will be carried out to confirm or rule out this statement.

Table 1 shows the results of the grain size, deformation percentage, and lattice parameter for the coatings produced. A decrease in crystallite size and lattice parameter was observed for samples with up to 2 silver pieces; however, for the samples with 3 and 4 silver inserts, no measurements were done, due to the fact that some peaks associated with silver and with the coatings are overlapped. Finally, in the peaks associated with stainless steel and with the coatings, the Ag signal tends to disappear, due to the amorphization effect, which is related to the high percentages of silver[31,32] located at grain boundaries. The SS FCC peak (220) is associated with the stainless steel substrate used to deposit the coatings.

Table 2 shows the results for the chemical composition of the deposited coatings, determined by means of the energy-dispersive X-ray spectroscopy (EDS) technique. In general, the EDS results show the presence of elements such as Fe, Cr, Ni, Mn, and Mo in percentages within the range in which austenitic stainless steels are found. The slight reduction of Mo in the coating with respect to the target is possibly due to the lower sputtering yield for this element, whereas the values of iron, nickel, and chromium have a higher yield[33]. Similarly, in the research carried out by Saker, A. et al., coatings of 310 stainless steel were deposited by means of the reactive triode DC magnetron sputtering technique, finding that the relative concentrations of some elements of the coating (Fe, Cr, and Ni) were different by less than 6% with respect to the composition of the target[34]. Regarding the coatings deposited with silver, an increase in the silver content was found as the number of pieces increased. In turn, a concomitant decrease in the contents was found for some of the elements of the coating (Cr, Mn, and Mo), which can be attributed to the increase in the number of Ag segments on the target, decreasing the effective sputtering area. The maximum percentage of Ag present in the coatings was 7.7 at.% for the coating deposited from a target with 4 Ag pieces.

The nanohardness results for the coatings show the high degree of hardness values obtained for the coatings with respect to the uncoated substrate. It should also be noted that the silver content slightly increases the hardness, which is in agreement with the results of investigations by other authors, who have found that at low concentrations of silver

Figure 4. X ray patterns of coating deposited.

as a doping material in nitride-type coatings, the hardness increases, and this has been explained by an increase in the film's density[35-38]. The increase in hardness can be attributed not only to the use of silver as a doping metal but also to the use of nitrogen in some of the layers that make up the coatings. The increase in hardness in the coatings deposited in a reactive atmosphere can be attributed to an increase in the lattice parameter and a percentage of deformation due to nitrogen supersaturation in the austenitic structure, also known as expanded austenite[10,11].

On the other hand, Table 2 shows the values of H/E and H^3/E^2, which do not exhibit a significant difference among the M0, M1, and M2 coatings; however, the M3 and M4 coatings, which have higher amounts of silver, exhibited higher H/E values. This could be considered to be an important parameter that influences the toughness of the coating. The Ag located at the grain boundary could dissipate the primary crack expanding energy and elevate the fracture resistance, and this favors a reduction of crack formation, deflection, and bridging at the grain boundary[16]. Nevertheless, soft silver exhibiting high toughness also contributed to the increase in the H/E ratio. Likewise, the coatings with higher percentages of silver exhibited a higher H^3/E^2 ratio, indicating that high percentages of silver contribute to an increase in the resistance to plastic flow of the coatings[39-42].

Figure 5 shows cross-section images of the M4 coating using SEM. In general, it can be seen as a compact structure with an absence of columnar growth. It is also important to note that despite the fact that the coatings were deposited in order to obtain a coating structure, it was not possible to observe them by means of the SEM technique. However, based on the deposition, the microstructure of the deposited films could be related to the T zone in zone models, and the silver nanoparticles are embedded in the steel-film crystal boundary[43]. Therefore, complementary studies using transmission electron microscopy are necessary.

Figure 6 shows the images that correspond to the wear tracks obtained by means of the scratch test technique in the coatings M0, M2, and M4. In general, it was not possible to determine the critical load, because there is no evidence of cohesive or adhesive failure, which is an indication of high adhesion of the coatings to the substrate, as well as a ductile characteristic of the coatings[44]. In the coatings M0 and M2, deformation mechanisms associated with the pile-up phenomena were observed, in which only the formation of burrs around the scratch track is in evidence[45,46]. In the case of coating M4, the formation of some semicircular cracks in the direction of the scratch was observed, representing a type of ductile tensile failure. As the test load increased, the density of the buckling cracks increased. In none of the cases were delamination characteristics observed[44]. In most cases, a single sample test was performed; however, in the cases in which repetitions were performed for the scratch tests, the same adherence behavior of the coatings to the substrate was identified, where it was not possible to identify the critical load and no delamination phenomena were observed.

Table 2. Chemical composition, hardness, and elastic modulus of coatings.

Sample	Silver pieces	Chemical Composition (at. %)						Hardness (GPa)	Elastic modulus (MPa)	H/E**	H^3/E^2 (GPa)
		Cr	Fe	Ni	Mn	Mo	Ag				
Target	NA	17.4	65.6	89	3.8	4.2	0.0	NA	NA	NA	NA
Subs. 316L	NA	16.4	69.9	10.1	1.5	2.1	0.0	2.8 ± 0.3	189± 15	0.015±0.003	0.001±0.001
M0	0	17.2	68.0	9.3	3.6	2.0	0.0	9.8±0.3	182±9	0.054±0.004	0.028±0.005
M1	1	16.6	68.5	9.4	2.8	2.0	0.6	10.4±0.2	192±9	0.054±0.003	0.031±0.004
M2	2	16.5	68.3	9.6	2.7	2.1	0.8	10.7±0.3	200±13	0.053±0.005	0.031±0.006
M3	3	16.4	67.0	9.6	2.8	2.1	2.2	11.1±0.4	192±10	0.058±0.005	0.037±0.008
M4	4	15.3	63.2	9.2	2.5	2.1	7.7	12.1±0.4	195±7	0.062±0.004	0.047±0.008

NA: Does not apply. H: Relation hardness. E: Elastic modulus.
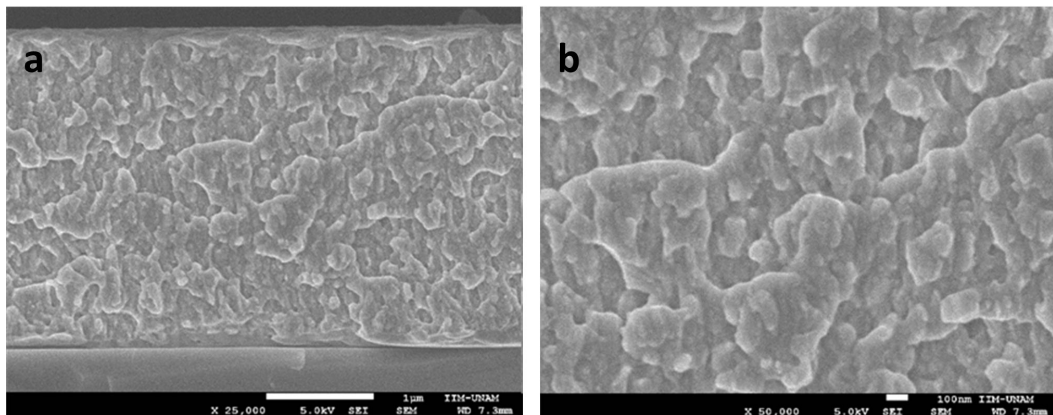
Figure 5. Cross-section SEM image of M4 coating. a) 25000X, b) 50000X.
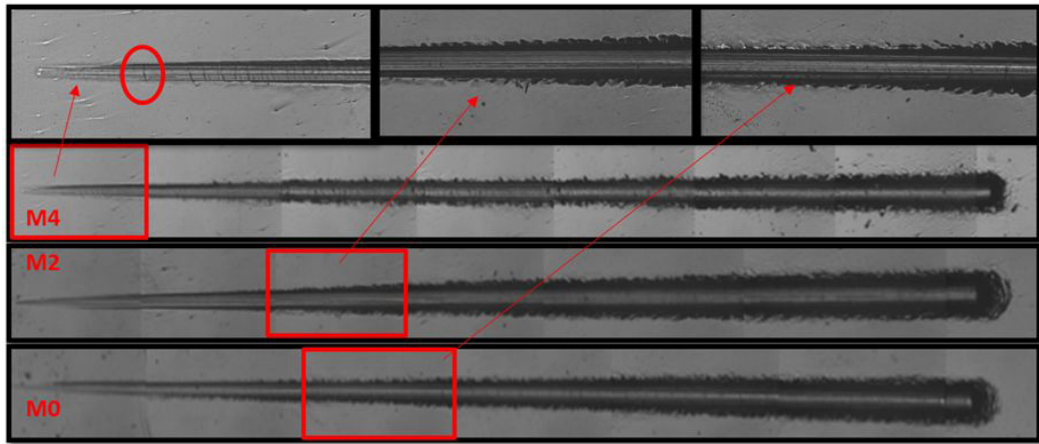
Figure 6. Optical microscopy of the scratch track of coating coatings M0, M2 y M4.

The values of the COF are shown in Figure 7. It can be seen that the coatings had a lower COF than that exhibited by the substrate. Additionally, it should be noted that the value of the friction coefficient decreased with the increase in the silver content. Silver is known to be a lubricating solid capable of reducing the COF value, since this material has a low resistance to shearing stresses[17], while steel film is characterized by its high values of hardness, which results in reducing the coefficient of friction. Likewise, the wear rate (see Figure 8) exhibited by the coatings was much lower than for the substrate. It was also found that as the percentage of silver in the coatings increased, the wear rate decreased. These results can be explained by the higher values of H/E and H^3/E^2 ratios in those materials. The higher values of the H/E ratio indicate that coatings are characterized by high toughness, which are represented by greater resistance to cracking as the percentages of silver increase. In the case of the H^3/E^2 ratio, higher values with respect to the substrate were also seen; in addition, when the silver content increases in coatings, the value of the H^3/E^2 ratio increases, indicating greater resistance to plastic deformation, and therefore greater resistance to wear, which was evidenced both in the COF values and in the wear rate. Furthermore, the combination of the high mechanical properties of the steel coating and the solid lubricating properties that silver possesses allowed lower wear rates compared to the coatings that did not contain Ag[16-18].

In Figure 9, the wear mechanisms exhibited by some of the tested samples can be observed by means of SEM. It can be seen that the coatings exhibited less damage caused by wear than did the substrate, the least being for the M4 coating, with higher silver content (Figure 9d). Oxidative wear mechanisms[21] can be seen both in the substrate and in the coatings, with the presence of an oxidized tribo-film on the surface, a result that can be confirmed with the results of the chemical composition of the wear track, determined by means of EDX, presented in Table 3, where the oxygen content in the wear marks as well as outside the wear marks is in evidence. In the same way, the contents of each of the elements of the stainless steel coatings and the percentage of silver (M3 and M4 samples) in each wear track are presented. Adhesive wear characteristics
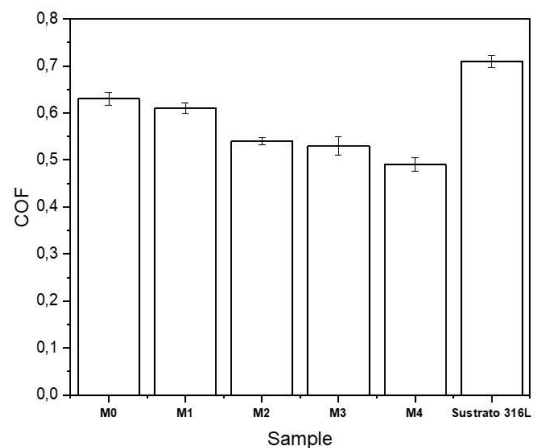

Figure 7. Coefficient of friction of the coatings and the substrate.
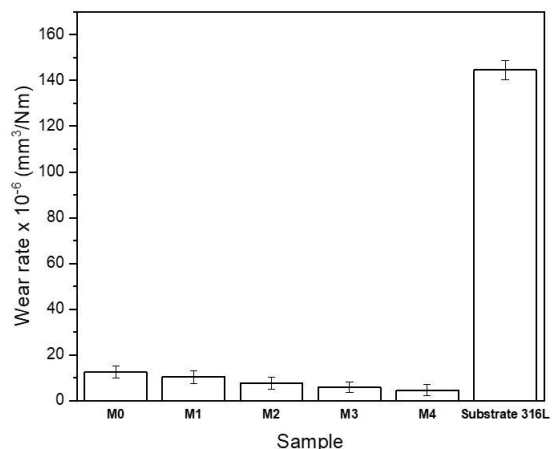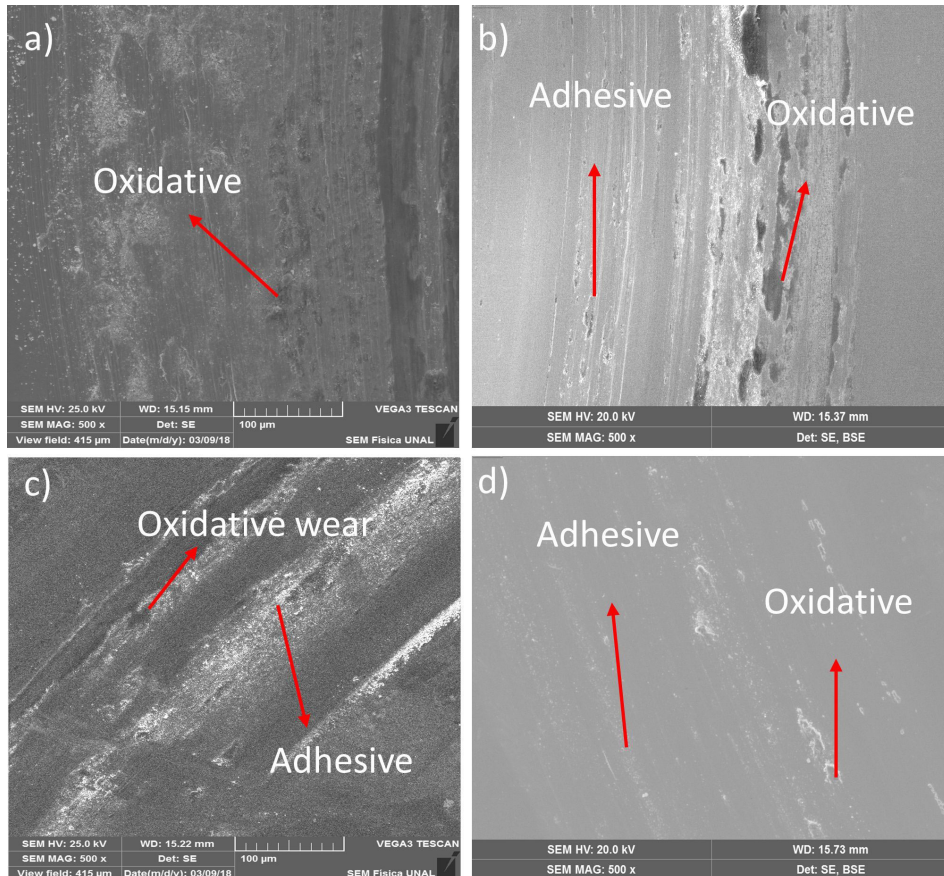

Figure 8. Wear rate of the coatings and the substrate.

were found in the coatings, which could be associated with the presence of material adhered to the surface of the tested samples[47,48]. No cracks or delamination of the coatings were observed in the wear tracks of the coatings.

Figure 9. SEM images of coating wear track. a) Substrate, b) M0, c) M3 and d)M4.

Table 3. Chemical composition of substrate wear track and coating obtained by EDX.

Sample	Chemical composition (at.%)						O (Without wear test)	O (With wear test)
	Fe	Cr	Ni	Mn	Mo	Ag		
Substrate 316L	41.33	10.56	5.51	0.82	0.33	-	16.35	41.25
M0	27.22	7.01	3.66	0.45	-	-	6.12	61.66
M3	49.24	12.50	6.52	0.32	0.38	0.75	0.00	30.03
M4	32.34	8.40	4.75	-	-	2.37	1.56	52.13

4. Conclusions

- Stainless steel coatings both without silver and with different silver contents were deposited. The coatings were grown in argon and argon-nitrogen (reactive atmosphere) by means of unbalanced magnetron sputtering.
- The coatings exhibited a combination of FCC and BCC crystalline structures, associated with the deposition of each layer in a reactive and an inert atmosphere, respectively. The FCC structure of silver was observed in the coatings deposited with a higher amount of silver, which also reduced the grain size.
- The chemical composition of the coatings showed evidence of the presence of elements such as Fe,

Cr, Ni, Mn, and Mo in percentages within the range in which austenitic stainless steels are found. The maximum percentage of Ag present in M4 coating was 7.7 at.%, deposited from a target with 4 Ag pieces.

- The coatings deposited with high silver content exhibited higher hardness values and an increase in the H/E and H^3/E^2 ratios. This contributes to an increase in the toughness and the resistance to plastic flow of the coatings produced with greater silver content.
- According to the COF and wear rate values, the best behavior against wear was exhibited by coatings with high percentages of silver. Regarding the wear mechanisms exhibited by the coatings, oxidative wear mainly prevailed.

5. Acknowledgements

6. References

1. Antunes Ra, Rodas CD, Lima NB, Higa OZ, Costa I. Study of the corrosion resistance and in vitro biocompatibility of PVD TiCN-coated AISI 316L austenitic stainless steel for orthopedic applications. Surf Coat Tech. 2010;205(7):2074-81.

2. Parsapour A, Khorasani SN, Fathi MH. Effect of surface treatment and metallic coating on corrosion behavior and biocompatibility of surgical 316L stainless steel implant. J Mater Sci Technol. 2012;28(2):125-31.

3. Gopi D, Ramya S, Rajeswari D, Kavitha L. Corrosion protection performance of porous strontium hydroxyapatite coating on polypyrrole coated 316L stainless steel. Colloids Surf B Biointerfaces. 2013;107:130-6.

4. Anghelina FV, Ungureanu DN, Bratu V, Popescu IN, Rusanescu CO. Fine structure analysis of biocompatible ceramic materials based hydroxyapatite and metallic biomaterials 316L. Appl Surf Sci. 2013;285:65-71.

5. Kannan S, Balamurugan A, Rajeswari S. Hydroxyapatite coatings on sulfuric acid treated type 316L SS and its electrochemical behaviour in Ringer's solution. Mater Lett. 2003;57(16-17):2382-9.

6. Bourjot A, Foos M, Frantz C. Basic properties of sputtered 310 stainless steel-nitrogen coatings. Surf Coat Tech. 1990;43-44:533-42.

7. Darbeida A, Saker A, Billard A, Von Stebut J. Optimization of the surface mechanical strength of AISI 31 6L physically vapour deposited nitrogen-doped coatings on AISI 31 6L substrates. . Surf Coat Tech. 1993;60:434-40.

8. Dahm KL, Betts AJ, Dearnley PA. Chemical structure and corrosion behaviour of S phase coatings. Surf Eng. 2010;26(4):271-6.

9. Sun Y, Kappaganthu SR. Effect of nitrogen doping on sliding wear behaviour of stainless steel coatings. Tribol Lett. 2004;17(4):845-50.

10. Schneider J, Rebholz C, Voevodin AA, Leyland A, Matthews A. Deposition and characterization of nitrogen containing stainless steel coatings prepared by reactive magnetron sputtering. Vacuum. 1996;47(9):1077-80.

11. Kappaganthu SR, Sun Y. Formation of an MN-type cubic nitride phase in reactively sputtered stainless steel-nitrogen films. J Cryst Growth. 2004;2671(1-2):385-93.

12. Kappaganthu S.R., Sun Y. Influence of sputter deposition conditions on phase evolution in nitrogen-doped stainless steel films. Surf Coat Tech. 2005;198(Spe 1-3):59-63.

13. Campoccia D, Montanaro L, Arciola CR. A review of the biomaterials technologies for infection-resistant surfaces. Biomaterials. 2013;34(34):8533-54.

14. Ávalos A, Haza M, Morales Y. Nanopartículas de plata: aplicaciones y riesgos tóxicos para la salud humana y el medio ambiente silver nanoparticles: applications and toxic risks to human heatlh and environment. Rev Complut Cienc Vet. 2013;7(2):1-23.

15. Taglietti A, Arciola CR, D'Agostino A, Dacarro G, Montanaro L, Campoccia D et al. Antibiofilm activity of a monolayer of silver nanoparticles anchored to an amino-silanized glass surface. Biomaterials. 2014;35(6):1779-88.

16. Velasco SC, Cavaleiro A, Carvalho S. Functional properties of ceramic-Ag nanocomposite coatings produced by magnetron sputtering. Prog Mater Sci. 2016;84:158-91.

17. Manninen NK, Ribeiro F, Escudeiro A, Polcar T, Carvalho S, Cavaleiro A. Influence of Ag content on mechanical and tribological behavior of DLC coatings. Surf Coat Tech. 2013;232:440-6.

18. Dang C, Li J, Wang Y, Yang Y, Wang Y, Chen J. Influence of Ag contents on structure and tribological properties of TiSiN-Ag nanocomposite coatings on Ti–6Al–4V. Appl Surf Sci. 2017;394:613-24.

19. Baranowska J, Fryska S, Przekop J, Suszko T. The properties of hard coating composed of S-phase obtained by PVD method. Adv Manuf Sci Technol. 2009;33(4):59-69.

20. Gutier P, Darbeı A, Billard A, Frantz C, Von Stebut J. Tribological behaviour of N- or O-doped austenitic stainless-steel magnetron sputter-deposited coatings. Surf Coat Tech. 1999;114(2-3):148-55.

21. Dahm K, Dearnley P. On the nature, properties and wear response of s-phase (nitrogen-alloyed stainless steel) coatings on AISI 316L. Proc Inst Mech Eng L: J Mater: Des Appl. 2000;214(4):181-98.

22. Klug H, Alexander L. X-ray diffraction procedures: for polycrystalline and amorphous materials. 2nd ed. Hoboken: Wiley; 1974.

23. ASTM International: American Society for Testing and Materials. Standard test method for wear testing with a pin-on-disk apparatus, G99. West Conshohocken: ASTM International;2006.

24. Ju H, He S, Yu L, Asempah I, Xu J. The improvement of oxidation resistance, mechanical and tribological properties of W2N films by doping silicon. Surf Coat Tech. 2017;317:158-65.

25. Baranowska J, Fryska S. Characterisation of mechanical properties of S-phase coatings produced by magnetron sputtering deposition. Chem Listy. 2011;105(17):769-72.

26. Kappaganthu SR, Sun Y. Studies of structure and morphology of sputter-deposited stainless steel-nitrogen films. Appl Phys, A Mater Sci Process. 2005;81(4):737-44.

27. Kuroda D, Hiromoto S, Hanawa T, Katada Y. Corrosion behavior of nickel-free high nitrogen austenitic stainless steel in simulated biological environments. Mater Trans. 2002;43(12):3100-4.

28. Terwagne G, Colaux J, Collins GA, Bodart F. Structural and quantitative analysis of nitrided stainless steel coatings deposited by dc-magnetron sputtering. Thin Solid Films. 2000;377:441-6.

29. Ferreri I, Lopes V, Calderon S, Tavares VCJ, Cavaleiro A, Carvalho S. Study of the effect of the silver content on the structural and mechanical behavior of Ag-ZrCN coatings for orthopedic prostheses. Mater Sci Eng C. 2014;42:782-90.

30. Sánchez-López JC, Abad MD, Carvalho I, Galindo RE, Benito N, Ribeiro S et al. Influence of silver content on the tribomechanical behavior on Ag-TiCN bioactive coatings. Surf Coat Tech. 2012;206(8-9):2192-8.

31. Siozios A, Zoubos H, Pliatsikas N, Koutsogeorgis DC, Vourlias G, Pavlidou E et al. Growth and annealing strategies to control the microstructure of AlN: ag nanocomposite films for plasmonic applications. Surf Coat Tech. 2014;255:28-36.

32. Aouadi SM, Debessai M, Filip P. Zirconium nitride/silver nanocomposite structures for biomedical applications. J Vac Sci Technol B Microelectron Nanometer Struct Process Meas Phenom. 2004;22(3):1134-40.

33. Godbole MJ, Pedraza AJ, Park JW, Geesey G. The crystal structures of stainless steel films sputter-deposited on austenitic stainless steel substrates. Scr Metall Mater States. 1993;28(10):1201-6.

34. Saker A, Leroy C, Michel H, Frantz C. Properties of sputtered stainless steel-nitrogen coatings and structural analogy with low temperature plasma nitrided layers of austenitic steels. Mater Sci Eng A. 1991;140(C):702-8.

35. Basnyat P, Luster B, Kertzman Z, Stadler S, Kohli P, Aouadi S et al. Mechanical and tribological properties of CrAlN-Ag self-lubricating films. Surf Coat Tech. 2007;202(4-7):1011-6.

36. Tseng CC, Hsieh JH, Wu W, Chang SY, Chang CL. Emergence of Ag particles and their effects on the mechanical properties

of TaN-Ag nanocomposite thin films. Surf Coat Tech. 2007;201(24):9565-70.

37. Huang HL, Chang YY, Lai MC, Lin CR, Lai CH, Shieh TM. Antibacterial TaN-Ag coatings on titanium dental implants. Surf Coat Tech. 2010;205(5):1636-41.

38. Aouadi SM, Bohnhoff A, Sodergren M, Mihut D, Rohde SL, Xu J et al. Tribological investigation of zirconium nitride/silver nanocomposite structures. Surf Coat Tech. 2006;201(1):418-22.

39. Ferreri I, Lopes V, Calderon S, Tavares VCJ, Cavaleiro A, Carvalho S. Study of the effect of the silver content on the structural and mechanical behavior of Ag-ZrCN coatings for orthopedic prostheses. Mater Sci Eng C. 2014;42:782-90.

40. Leyland A, Matthews A. On the significance of the H/E ratio in wear control: a nanocomposite coating approach to optimised tribological behaviour. Wear. 2000;246(1-2):1-11.

41. Hoeppner DW. Structural integrity considerations in engineering design. London: Imperial College Press;2011.

42. Holmberg K, Matthews A. Coatings tribology: properties, mechanisms, techniques and applications in surface engineering. Amsterdam: Elsevier Science;2009.

43. Martín JMA, editor. Láminas delgadas y recubrimientos: preparación, propiedades y aplicaciones. Madrid: CSIC Press;2003.

44. Fryska S, Słowik J, Baranowska J. Structure and mechanical properties of chromium nitride/S-phase composite coatings deposited on 304 stainless steel. Thin Solid Films. 2019;676:144-50.

45. Bull SJ. Failure mode maps in the thin film scratch adhesion test. Tribol Int. 1997;30(7):491-8.

46. Kuiry S. Advanced scratch testing for evaluation of coatings. Tribology and mechanical testing. Santa Barbara: Bruker Nano Surfaces Division; 2012.

47. Gilewicz A, Warcholinski B. Tribological properties of CrCN/CrN multilayer coatings. Tribol Int. 2014;80:34-40.

48. Rasool G, Stack MM. Wear maps for TiC composite based coatings deposited on 303 stainless steel. Tribol Int. 2014;74:93-102.